Assessment of Intermetallic Compounds within Dissimilar Joints Using Nonlinear Guided-Wave Features

MIMA MANSOUR, MOHAMMAD ALI FAKIH, FADI AL-BADOUR and SAMIR MUSTAPHA

ABSTRACT

The welding of dissimilar materials finds a wide variety of applications in the fields of industrial construction and manufacturing. One of the most prominent challenges of these techniques is the development of intermetallic compounds (IMCs) at the joint level, which reduces the strength of the welds. Nonlinear ultrasound detection methods are used as modern non-destructive testing tools for inspecting early damage in various materials. This study investigates the assessment of the thickness of the IMC layer within dissimilar joints using non-linear guided-wave (GW) features. A numerical investigation was performed on friction-stir-welded (FSW) lap joints, between AA5052-H32 aluminum and ASTM 516-70 steel, with various intermetallic conditions/thicknesses. GWs were excited in the specimens using piezoelectric transducers placed on the aluminum side. The second-harmonic generation (SHG) among the fundamental GW modes was examined within the low-excitation-frequency range. It was found that the relative acoustic nonlinearity parameter β' varies linearly with the thickness of the IMC layer. The attained results prove the sensitivity of GW nonlinear features to microstructural variations, within dissimilar FSW joints, and demonstrate the capability of LWs in accurately scrutinizing their strength.

Keywords: Friction stir welding, dissimilar welds, intermetallic compound, nonlinear guided waves, acoustic non-linear parameter, numerical modelling.

Mirna Mansour and Samir Mustapha, Laboratory of Smart Structures and Structural Integrity (SSSI), Department of Mechanical Engineering, American University of Beirut, Beirut, Lebanon.

Mohammad Ali Fakih, Institute of Fluid-Flow Machinery, Polish Academy of Sciences, 80-231 Gdańsk, Poland.

Fadi Al-Badour, Mechanical Engineering Department, King Fahd University of Petroleum and Minerals, 31261 Dhahran, Saudi Arabia.

INTRODUCTION

Structural Health Monitoring (SHM) systems have gained significant attention from researchers and engineers in various engineering fields due to the importance of continuously monitoring and evaluating engineering structures. SHM technologies greatly impact the performance of structures by enhancing their safety and reducing maintenance inspections and repair costs [1].

Dissimilar materials joining can be described as combining materials that are often more difficult to join than pieces of the same material or alloys with minor differences in composition [2]. One of the most important challenges of dissimilar-metal welding is the development of intermetallic compounds (IMCs) at the joint level. The presence of IMCs reduces the bonding strength causing low fracture toughness, hence accelerating the formation of cracks and voids [3].To evaluate the quality of structural components during manufacturing and throughout their service life, various non-destructive testing (NDT) methods have been developed and commonly used, including visual inspection, tapping, thermography, radiography, eddy-current, electromagnetic, electromechanical, and ultrasonic analysis [4, 5]. Guided waves, in particular, have demonstrated their effectiveness and have been widely used in developing damage identification algorithms to assess fatigue cracking, delamination, fiber breakage, and corrosion in composite and metallic structures over the past few decades [6]. Nonlinear guided-wave features have a strong potential to shift the paradigm in the lifecycle management of structural systems because they can provide indications of incipient material damage [7].

Zhu et al. [8] have used the static component of Lamb waves (SCLWs), a secondary wave that emerges at different frequencies as a result of the self-interaction of primary LWs, to detect a closed crack in an aluminum alloy. It was found that the acoustic nonlinearity parameter of SCLWs, A_0/A_1, increases with the crack length and orientation angle and decreases with the crack width. Aslam et al. [9] studied defect-localization techniques using the nonlinear interaction between primary Lamb wave modes. The results show that the sensitivity of nonlinearity due to crack wave interaction increases when Lamb wave mixing occurs at the fault zone. Zhao et al. [10] used the third-harmonic amplitude and third-order nonlinear LW parameters to experimentally detect early fatigue damage in aluminum alloys. The third-order nonlinear parameters have been identified as effective indicators. It was noticed that the amplitude of the wave's third-harmonic component increases when the fatigue life falls below about 80%. Lee et al. [11] studied and identified fatigue cracks in a steel joint using nonlinear guided waves through second harmonic generation using piezoelectric transducers. It is observed that the percent of the reduction in nonlinearity increased with crack growth. Further, Fakih et al. [12] used second-order nonlinear parameters for the detection and evaluation of micro-scaled intermetallic compounds (IMCs) in friction stir welding lap joints, between AA5052-H32 aluminum and ASTM 516-70 steel, with various intermetallic conditions numerically. The authors used a high excitation frequency and they found that the relative acoustic nonlinearity parameter varies linearly with the thickness of the IMC layer.

This paper investigates the impact of intermetallic compounds on guided waves in dissimilar friction stir welds, which has not been studied in the literature using low frequency. Specifically, the study uses the GW nonlinearity to assess IMCs

in simulated dissimilar FSW lap joints between AA5052-H32 aluminum and ASTM 516-70 steel, which contain IMCs of varying thicknesses.

METHODOLOGY

Nonlinear Parameter

The intrinsic nonlinearities of an elastic medium and any potential resulting nonlinearities cause distortions in an ultrasonic wave as it travels through the medium. This can result in a variety of nonlinear components, such as sub-harmonics (which are produced at fractional multiples of the excitation/fundamental frequency), higher-order harmonics that are also known as super-harmonics, or mixed frequencies that modulate the interrogating wave [13]. Second-order harmonics of LWs in particular, have drawn the attention of many researchers in recent decades due to their demonstrated sensitivity to microstructural changes and degradation in both composite and metallic structures. The displacement of the fundamental frequency and second-order harmonic frequency components of the propagated ultrasonic wave defines the nonlinearity parameter, also known as the absolute nonlinearity parameter [13] that is calculated using equation (I).

$$\beta' = \frac{A_2}{A_1^2} \tag{I}$$

To ensure a signal-to-noise ratio (SNR) in cumulative second-harmonic generation, it is important to selectively stimulate Guided waves at specific frequencies. This is due to the relatively weak amplitudes of the second-harmonic modes. To achieve this, two conditions must be met: firstly, the phase velocity of the fundamental wave mode at the excitation frequency should be equal (or close to it) to the phase velocity of another mode at twice the excitation frequency. Secondly, there should be a non-zero power flux between these modes. By satisfying these conditions, it becomes possible to generate second-harmonic signals effectively while maintaining a high SNR.

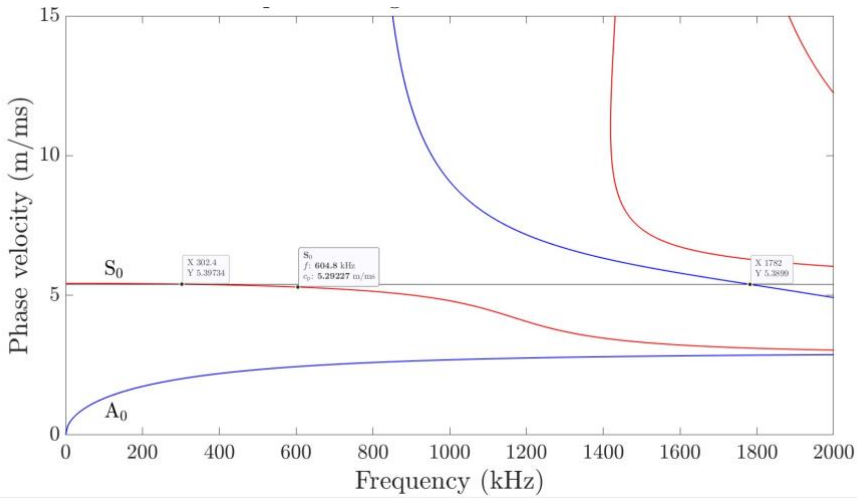

Figure 1. Dispersion curve of LW modes in a 2-mm thick AA5052-H32 aluminum plate [14].

Figure 1 displays the theoretical phase velocity dispersion curve for a 2-mm thick AA5052-H32 aluminum plate (that is used in the current study) determined by the dispersion calculator. Guided waves are excited in the models using PZT transducers with a central excitation frequency of 300 kHz (because we are aiming for low frequencies) to meet the synchronism and zero-flux conditions of second-harmonic generation, as indicated in Figure **1**.

FINITE ELEMENT MODEL

The work of Ibrahim et al. [15], in which the microstructural and mechanical characteristics of friction stir diffusion cladding (FSDC) samples were thoroughly studied, served as the basis for our investigation. FSDC is a newly developed cladding technique similar to FSW lap welding where the entire cladding surface is processed. One-pass FSDC joints between 2-mm AA5052-H32 aluminum and 7-mm ASTM 516-70 steel samples are shown in Figure 2. EDS line-scan analysis was used to characterize the diffusion zone, which defines the interface between the two materials, and the composition variation technique was used to measure the interface thickness shown in Figure 3. Table I shows the different welding-process parameters that caused a variation in the interface thickness between the specimens.

COMSOL® Multiphysics was used to create a 2D plane-strain model for the AA5052-H32/ASTM 516-70 lap weld [12], as shown in

Figure **4**. The finite element (FE) model includes an AA5052-H32 plate with a 2-mm thickness and 56-mm length on top of an ASTM 516-70 plate with a 7-mm thickness and 55-mm length. Based on the width of the accessible specimens, the model's width was determined to be 12 mm (Table I). The Murnaghan nonlinear-elastic material model was used. On the left edge of the aluminum plate, one PZT actuator (7 mm in length and 0.5 mm in thickness) was mounted and was modeled using a solid-mechanics/electrostatics multi-physics solver. The PZT wafer was fed with the 15.5-cycle Hann-windowed sinusoidal excitation signals after trying different excitation frequencies using low frequencies to meet the two conditions of synchronism using 240-V peak-to-peak voltage. We reproduced intermetallic regions in the FE model by adjusting the material properties of several interface sub-layers. These sub-layers, each measuring 2 μm in thickness and 21.5 mm in length and were modified within the welded region between the two materials. Insets of the zoomed-in weld region in

Figure **4** display the employed interface sublayers. Six alternative models, one without IMCs and the other five with 2-, 4-, 6-, 8-, and 10 μm IMC layers, were used to build six possible scenarios for the presence of IMC. To ensure a minimum of 9 elements per wavelength of the A_0 mode (using a dispersion calculator), a free quadrilateral mesh was utilized in the aluminum sub-plate with an element size limit of approximately 0.135 mm. Rectangular elements with a size of 0.002×0.02 mm² were employed to enable correct meshing of the micro-sized interface sub-layers. This has generated a very fine mesh within the weld region, with element sizes in the order of a few μm. After about 3.5 mm just below the weld interface, the mesh size was loosened up to a maximum element size of about 1.35 mm at the bottom edge of the steel sub-plate. The overall simulation period was set to t = 200 μs, and U_1 displacements were determined using a set

of 37 sensing points that were evenly spaced throughout the upper surfaces of both sub-plates using a sampling rate of 100 MHz. The sensing points were positioned over a range of 8 to 80 mm from the left border of the model at 2 mm intervals. The model's bottom right corner was fixed to restrict its movement.

The interface layers were treated as homogeneous isotropic linear-elastic materials due to the uncertainty surrounding the precise composition and material characteristics of the interface layers and the difficulty in obtaining the nonlinear-elastic properties of IMCs. The Energy dispersive spectroscopy (EDS) characterization of interface layers (Figure 3) demonstrates a smooth transition from steel to aluminum compositions, with the composition percentage of steel against aluminum (and vice versa) varying in a rather linear manner inside the interface layer. As a result, a method of dividing the IMC layer into many sub-layers, each of 2μm thickness, is suggested. The physical and mechanical properties of the sub-layers were assumed using linear interpolation between those of aluminum and steel.

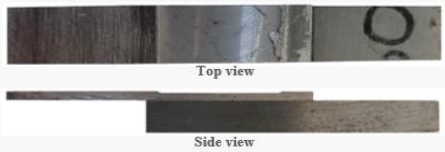

Material	Density (kg/m³)	Lame parameters (GPa)		Murnaghan ToE constants (GPa)		
		λ	μ	l	m	n
AA5052-H32	2680	51.3	26.4	-252	-325	-351
ASTM 516-70	7800	107.05	77.5	-248	-623	-714

Figure 2. (a) The different specimens and their top and side view [15], and (b) show the properties of the different specimens.

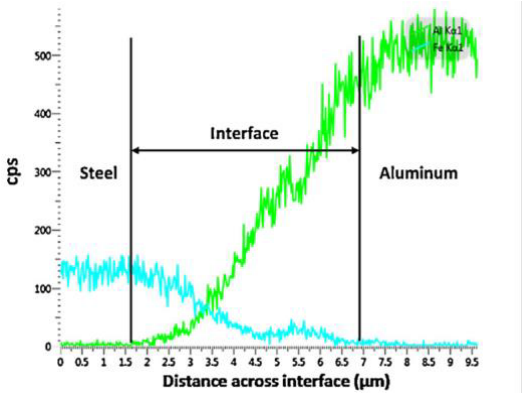

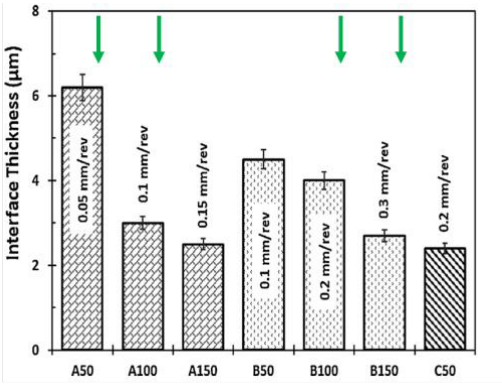

Figure 3. (a) EDS line scan analysing the interface layer thickness, and (b) shows the interface-layer thickness (in μm) of different specimens [15].

Table I. Geometry and variable welding parameters of the available FSDC specimens [15].

Name	Number of available specimens	Length (mm)	Width(mm)	Tool's rotational speed (RPM)	Tool's feed speed (m/s)
A50	2	80	12-12.5	1000	50
A100	1	80	11	1000	100
B100	1	80	19	500	100
B150	2	80	12.3-15	500	150

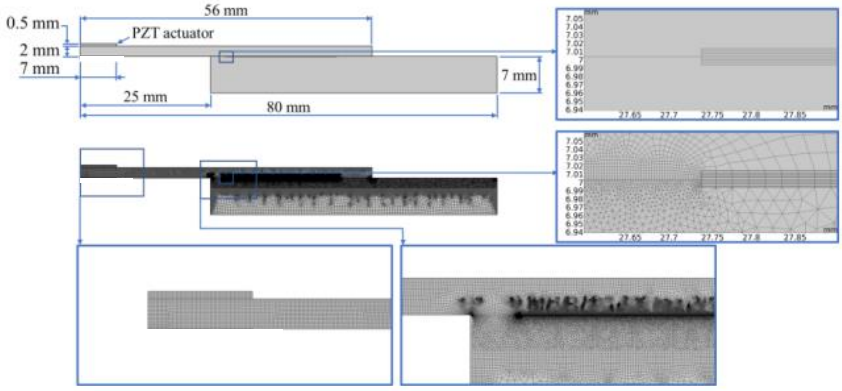

Figure 4. Geometry and mesh of the AA5052-H32/ASTM 516-70 lap-weld 2D plane-strain FE model [12].

SPECTRAL AND NONLINEARITY ANALYSIS

Second-Harmonic Generation (SHG)

After the waveform response had been obtained from the sensors, an analysis of the raw data was performed. To investigate the presence of second-harmonic generation and analyze the frequency content of the measured time-domain signals, the signals were transformed to the frequency domain using the fast Fourier transform (FFT). When the excitation frequency was set to 300 kHz, the FFT displayed a second-harmonic component, with multiple peaks observed around the nearest peak (Figure 5). Due to the large amplitude difference between the fundamental and second-harmonic frequencies, the FFT plot was divided into two plots that displayed the $F_e$and $2F_e$ domains separately. To observe the cumulative SHG over the propagation distance, β' was plotted versus the sensor positions as shown in Figure 6. β' was slightly increasing from 9 to 24 mm (just before the beginning of the steel plate). After entering the steel plate β' starts to increase in a relatively linear manner from 25 to 56 mm. Beyond 56 mm, after the end of the aluminum plate where the waves were measured on the surface of the steel plate, a sharp and random variation is observed.

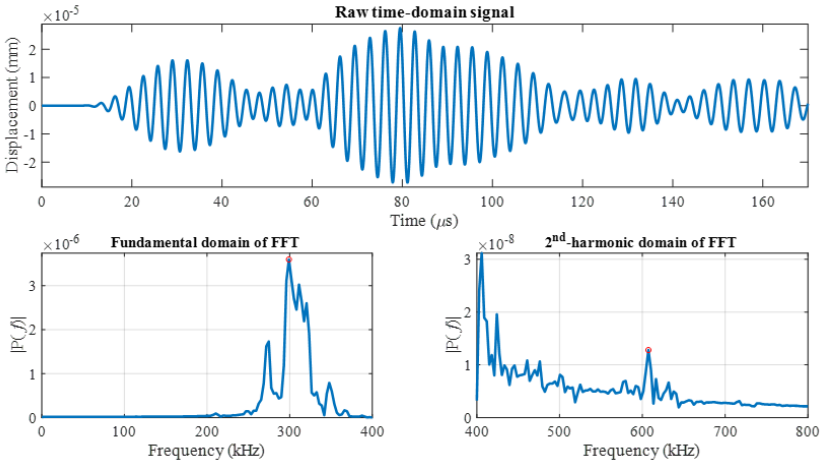

Figure 5. A typical raw signal in the time and frequency domain measured at sensor position = 30 mm using an excitation frequency of 300 kHz while exiting from the aluminum side.

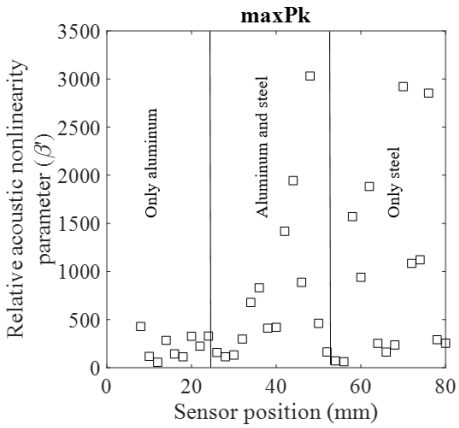

Figure 6. β' versus the sensor positions in the dissimilar lap-weld model while exciting from the aluminum side.

ASSESSMENT OF INTERMETALLIC COMPOUNDS

A series of measurements were taken at various sensing positions from dissimilar lap-weld models, each containing a different thickness of the intermetallic-compound layer. The objective of this is to determine the effectiveness of the SHG technique in detecting the slightest variations in the IMC layer thickness within the welded joint. β' was calculated for each model at every sensing position. The resulting data was then used to plot the variation of the average β' with the thickness of the IMC layer in the lap joint region, presented in Figure 7**.** Each point on the plot represents the average value of β' for each sample within the welded part (from sensing point 24 mm to 56 mm). We can see that β' slightly decreases linearly as the thickness of the intermetallic layer increases. The study concluded that the SHG technique can successfully detect very small variations in the thickness of the IMC layer, despite the possible sources of the SHG within the measured waves. Moreover, a linear correlation was identified between β' and the thickness of the IMC layer, indicating the potential use of β' in performing a quantitative assessment of such microstructures.

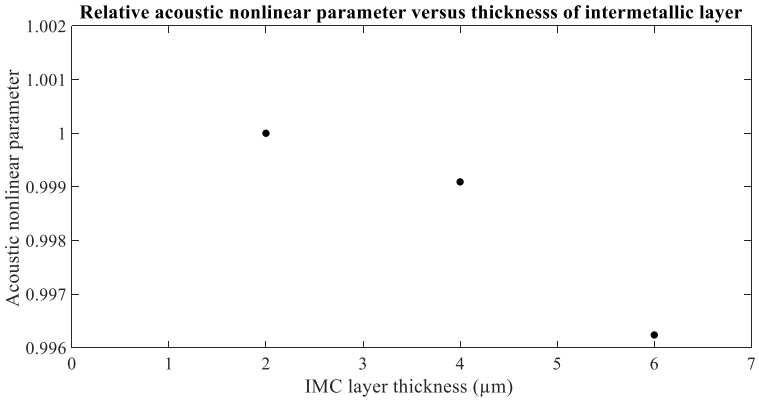

Figure 7. Variation of the average acoustic nonlinear parameter β' versus the thickness of the intermetallic layer within the welded joint.

CONCLUSIONS

This study showed the potential of Lamb-wave nonlinear features, namely the second-harmonic generation, for the quantitative assessment of micro-scaled intermetallic compounds within the interface region of a dissimilar welded joint. A finite element model was built for an AA5052-H32/ASTM 516-70 lap-weld. Guided waves were excited within the model, based on the synchronism and zero-flux conditions of second-harmonic generation. The relative acoustic nonlinearity parameter (β') was calculated at different sensing positions. The variation of average β', upon the presence of the IMC layers (of various thickness and material properties) in the lap-weld interface, was then scrutinized. It was demonstrated that the nonlinearity parameter, calculated from signals measured within the welded region, decreases linearly with the increase of the IMC-layer thickness. This proves the capability of nonlinear Lamb-wave features, and specifically the second-harmonic generation, of the quantitative evaluation of micro-scaled damage or microstructural variations within dissimilar welded joints.

REFERENCES

1. Brownjohn, J., *Structural health monitoring of civil infrastructure.* Philosophical transactions. Series A, Mathematical, physical, and engineering sciences, 2007. **365**: p. 589-622.
2. da Cunha, T.V. and C.E.N.J.U. Bohórquez, *Ultrasound in arc welding: a review.* 2015. **56**: p. 201-209.
3. Albannai, A.J.I.J.S.T.R., *Review the common defects in friction stir welding.* 2020. **9**: p. 318-329.
4. Sohn, H.J.P.T.o.t.R.S.A.M., Physical and E. Sciences, *Effects of environmental and operational variability on structural health monitoring.* 2006. **365**: p. 539 - 560.
5. Park, G., et al., *Energy harvesting for structural health monitoring sensor networks.* 2008. **14**(1): p. 64-79.
6. Mustapha, S., et al., *Evaluation of barely visible indentation damage (BVID) in CF/EP sandwich composites using guided wave signals.* 2016. **76**: p. 497-517.
7. Jhang, K.-Y. and K.-C. Kim, *Evaluation of material degradation using nonlinear acoustic effect.* Ultrasonics, 1999. **37**(1): p. 39-44.
8. Zhu, W., et al., *Nonlinear ultrasonic detection of partially closed cracks in metal plates using static component of lamb waves.* 2021. **124**: p. 102538.
9. Aslam, M., P. Nagarajan, and M.J.J.o.N.E. Remanan, *Defect localization using nonlinear Lamb wave mixing technique.* 2021. **40**(1): p. 1-12.

10. Zhao, G., et al., *Early fatigue damage evaluation based on nonlinear Lamb wave third-harmonic phase velocity matching.* 2022: p. 107288.
11. Lee, Y.F. and Y. Lu, *Identification of fatigue crack under vibration by nonlinear guided waves.* Mechanical Systems and Signal Processing, 2022. **163**: p. 108138.
12. Fakih, M.A., *Condition Assessment of Dissimilar Friction-Stir-Welded Joints Using Ultrasonic Lamb Waves*. 2021.
13. Hong, M., et al., *Locating fatigue damage using temporal signal features of nonlinear Lamb waves.* 2015. **60**: p. 182-197.
14. Huber, A., *Dispersion Calculator.* 2018.
15. Ibrahim, A.B., et al., *Effect of process parameters on microstructural and mechanical properties of friction stir diffusion cladded ASTM A516-70 steel using 5052 Al alloy.* 2018. **34**: p. 451-462.